Role of the integrin-β1/TGF-β1 signaling pathway in the pathogenesis of pelvic organ prolapse: A study on vaginal wall tissue alterations and molecular dysfunction

MIN KONG[1,2*], ZHUO WANG[1,2*], YAO HAO[3,4], YUEYUE SHI[1,2], XIN YANG[1,2], NGENZI RICHARD DJURIST[1,2] and YAN LI[1]

[1]Department of Gynecology, General Hospital of Ningxia Medical University, Yinchuan, Ningxia Hui Autonomous Region 750004, P.R. China; [2]School of Clinical Medicine, Ningxia Medical University, Yinchuan, Ningxia Hui Autonomous Region 750004, P.R. China; [3]School of Basic Medical Sciences, Ningxia Medical University, Yinchuan, Ningxia Hui Autonomous Region 750004, P.R. China; [4]Key Laboratory of Fertility Maintenance, Ministry of Education, Yinchuan, Ningxia Hui Autonomous Region 750004, P.R. China

Received August 18, 2024; Accepted December 12, 2024

DOI: 10.3892/mmr.2025.13469

Abstract. Pelvic organ prolapse (POP) is a prevalent condition among middle-aged and older women, and is associated with the irregular production and breakdown of the extracellular matrix. Mechanical forces serve a key role in preserving the equilibrium between matrix synthesis and degradation, thereby supporting the structural integrity of pelvic floor tissues. The aim of the present study was to investigate alterations in the composition of vaginal wall tissues in individuals suffering from POP and to investigate the molecular mechanisms through which mechanical forces trigger fibroblast apoptosis and influence collagen expression via the integrin-β1/TGF-β1 signaling pathway. Masson's trichrome and Elastica van Gieson staining were used to examine the pathological alterations in the tissue associated with POP. Analysis of immunofluorescence, western blotting and reverse transcription-quantitative PCR data was performed to assess changes in the levels of proteins and genes such as collagen, integrin-β1, TGF-β1, MMP-1 and tissue inhibitor of metalloproteinase-1 (TIMP-1). Fibroblasts were incubated with an integrin-β1 antagonist RGD peptide to mimic cellular injury induced by mechanical forces, and cell migration and apoptosis were analyzed using scratch assays and flow cytometry. Cytoskeletal alterations were detected via immunofluorescence staining, and western blot analysis was conducted to examine the expression levels of integrin-β1, TGF-β1, TIMP-1, MMP-1, collagen type I α1 chain (COL1A1) and collagen type III α1 chain (COL3A1) across various groups. Analysis revealed that in the POP group, the collagen fibers in the vaginal wall tissues were loose and irregularly arranged, the number of elastic fibers was reduced and the structure was degraded. Furthermore, stress fibers were incomplete and their functions were impaired, resulting in damage to the connective tissue structure of the pelvic floor. Integrin-β1 was key for fibroblast migration, apoptosis and collagen synthesis. Additionally, the integrin-β1/TGF-β1 signaling pathway served a role in mediating fibroblast apoptosis, and influencing the synthesis and metabolism of COL1A1 and COL3A1 induced by mechanical forces. Understanding the underlying pathogenesis of pelvic floor organ prolapse could pave the way for future investigations into innovative prevention and treatment strategies.

Correspondence to: Professor Yan Li, Department of Gynecology, General Hospital of Ningxia Medical University, 804 Shengli Street, Xingqing, Yinchuan, Ningxia Hui Autonomous Region 750004, P.R. China
E-mail: zyy02386@nxmu.edu.cn

*Contributed equally

Key words: pelvic organ prolapse, collagen, fibroblasts, integrin-β1, transforming growth factor-β1

Introduction

Pelvic organ prolapse (POP) is a common disease in middle-aged and elderly women (1). For various reasons (2,3), including vaginal delivery, parity, birthweight, age and body mass index, the position of the pelvic organs can drop and protrude into the vagina or even protrude from the vaginal opening, resulting in abnormal organ position and function. POP is a multifactorial disease in which age is an independent risk factor and pregnancy is the most common risk factor for disease development, as vaginal birth can damage the pelvic floor muscles and connective tissues (4). In addition, high estrogen levels before hysterectomy, multiple pregnancies, increased age, increased BMI and persistently increased intra-abdominal pressure (including obesity, chronic cough, constipation and repeated weight-bearing) may also lead to prolapse (5). At present, the incidence of POP is increasing annually, and surgery is still the most common treatment method for patients with severe POP (6). A community physical examination in the Netherlands revealed that 75% of women aged 45-85 years had POP, with 10-20% of these women requiring surgical treatment (7). Large-sample

epidemiological surveys in China have revealed that 43-76% of patients with POP require surgical treatment and that ~1/3 of patients with POP who receive surgical treatment require secondary surgical treatment (8-10). A projection in the United States revealed that the number of patients undergoing pelvic floor surgery for POP will increase from ~170,000 in 2010 to ~250,000 by 2050 (11). Although POP is not a fatal disease, it can reduce patient quality of life and even cause serious psychosocial problems (1). The molecular biological mechanisms of POP have become hot research topics.

The female pelvic floor is subjected to tension caused by pregnancy, childbirth or defecation amongst other causes, which increases abdominal pressure (12). The supporting function of the pelvic floor connective tissue mainly depends on the extracellular matrix (ECM). Changes in the degradation and composition of the ECM can disrupt the mechanical balance of the pelvic floor connective tissue, and serve a key role in the occurrence and development of POP (13). The main components of the ECM are collagen and elastin, and the metabolism of collagen and elastin is regulated by fibroblasts (14). A study has shown that mechanosensitive pathways serve a key role in fibroblast activation (15). Fibroblasts sense mechanical forces through mechanosensitive receptors, including integrins, ion channels, G protein-coupled receptors and growth factor receptors, and mediate responses to mechanical stress (16). Integrins are cell membrane surface receptors that mainly mediate adhesion between cells, and between cells and the ECM; they are also important mechanical signal receptors (17). One study showed that integrin-mediated adhesion can enhance TGF-β1-induced signal transduction (18). Loss of integrin α1β1 leads to increased TGF-β-mediated signaling and unilateral ureteral obstruction fibrosis, while TGF-β-mediated activation of classical signaling is the main driver of tubular renal fibrosis in integrin α1 knockout mice. It can be seen that the two signaling pathways mediated by integrins and the TGF-β1 receptor can be coupled through their downstream signaling molecules (19). It is unclear whether integrins also alter TGF-β profibrotic signaling by directly modulating the activity of the TGF-β receptors complex.

A study has shown that, after myocardial infarction, αvβ5 integrin expression is upregulated in fibroblasts (20). Perrucci *et al* (21) reported that αvβ5 integrin expression levels were also upregulated in cardiac fibroblasts from spontaneously hypertensive rats. *In vitro* inhibition by cilengitide could effectively prevent the differentiation of cardiac fibroblasts into myofibroblasts in spontaneously hypertensive rats. These findings suggest the possibility of treating cardiac fibrosis with the integrin αvβ5 inhibitor cilengitide (21). In addition, several studies have shown that mechanical force can affect the expression levels of integrin-β1 in the sacral ligaments of patients with POP (22), thereby exerting an adaptive effect on cytoskeletal morphology (23). However, to the best of our knowledge, there is currently no research on the regulation and mechanism of integrins by mechanical signals. Therefore, the aims of the present study were to investigate the mechanism by which mechanical force affects collagen synthesis and metabolism through integrin-β1/TGF-β1 and to provide a novel direction for the prevention and treatment of POP.

Materials and methods

Ethical statement. All procedures involving human samples in the present study were conducted with ethics-approved protocols in accordance with the guidelines of the Ethics Committee of Ningxia Medical University (approval no. KYLL-2024-0223; Yinchuan, China). All patients signed informed consent forms prior to surgery.

Source of the samples. Samples were collected from 20 patients aged 45-70 years with POP-Q stages III-IV (24) who underwent total hysterectomy for uterine and anterior vaginal wall prolapse at Ningxia Medical University General Hospital (Yinchuan, China) between March and December 2022. The inclusion criteria included: Confirmed POP diagnosis, elective hysterectomy and informed consent. The exclusion criteria included: Gynecological malignancies, prior pelvic radiation or incomplete records. The control group consisted of 20 patients aged 45-70 years who underwent total hysterectomy for benign gynecological conditions such as leiomyomas and adenomyosis at the same hospital during the same period. The inclusion criteria included a diagnosis of benign disease with no history of POP, with the same exclusion criteria as the POP group. All patients included in the present study did not have urinary incontinence, had not undergone hormone replacement therapy within 3 months prior to surgery and had no history of endometriosis. Additionally, none of the patients presented with respiratory, cardiovascular, skin or other connective tissue abnormalities that could influence cytoskeletal metabolism. There were no statistically significant differences between the two groups in terms of age, number of pregnancies, number of vaginal deliveries or BMI ($P>0.05$; Table I).

Tissue specimen preparation. Discarded vaginal wall tissue removed by surgery was obtained. All layers were intact, and the size of each specimen was ~1 cm^3. After rinsing with sterile saline, the specimens were fixed in 4% paraformaldehyde solution for 24 h at 4˚C. A portion of each tissue was dehydrated with 30% sucrose and then embedded in optimal cutting temperature compound. Frozen sections (12-μm thick) were prepared at -20˚C for immunofluorescence experiments. The remaining portion of the tissue was dehydrated using an ascending alcohol gradient, cleared, embedded in paraffin and cooled. The tissue was serially sectioned at a thickness of 5-μm and then used for the next step of staining.

Masson's trichrome and Elastica van Gieson (EVG) staining. For Masson staining (Beijing Solarbio Science & Technology Co., Ltd.), the paraffin sections were dewaxed, stained with hematoxylin for 8 min at room temperature, rinsed with running water and differentiated with 1% hydrochloric acid for 1 min. The sections were rinsed with running water for 1 min, stained with Masson staining solution at room temperature for 8 min and rinsed with distilled water for 1 min. Subsequently, the sections were treated with 1% phosphomolybdic acid solution for 5 min, counterstained with aniline blue solution for 5 min and treated with 1% glacial acetic acid for 1 min (all at room temperature). Afterwards, the sections were dehydrated with 95% alcohol and absolute ethanol, made transparent with xylene, and sealed with neutral gum. For EVG staining

Table I. Comparison of general conditions of control subjects and patients with POP.

Variable	Control (n=20)	POP (n=20)	P-value
Age, years (mean ± SD)	58.45±4.89	60.20±8.29	0.42
BMI, kg/m^2 (mean ± SD)	25.90±4.16	24.03±1.45	0.07
Median number of pregnancies (range)	3.00 (0-5)	4.00 (2-13)	0.12
Median number of vaginal deliveries (range)	2.00 (0-4)	2.50 (1-10)	0.16

POP, pelvic organ prolapse.

(Beijing Solarbio Science & Technology Co., Ltd.), the paraffin sections were dewaxed, stained with modified VG staining solution for 10 min, and washed with distilled water for 10 sec to wash away excess dye. Verhöeff staining working solution was added dropwise for 5 min, and sections were washed with distilled water for 10 sec. The Verhoeff differentiation solution was used for differentiation for 10 sec until the elastic fibers were clear. The seconds were washed for 10 sec with distilled water. Gradient ethanol dehydration was performed starting from 75% ethanol (5 sec each time). Sections were cleared with xylene twice for 1 min each, and the slide was sealed with neutral gum. The aforementioned steps were performed at room temperature. The images were viewed under a Nikon Eclipse E100 light microscope (Nikon Corporation).

Immunofluorescence staining. Frozen tissue sections were thawed and washed three times with PBS, permeabilized with 0.3% Triton-100 (Beijing Solarbio Science & Technology Co., Ltd.) for 30 min, blocked with 10% goat serum (Beyotime Institute of Biotechnology) at room temperature for 40 min, and incubated with the primary antibodies overnight at 4˚C. Cells were fixed with 4% paraformaldehyde at room temperature for 30 min, washed three times with PBS and permeabilized with 0.5% Triton-100 (Beijing Solarbio Science & Technology Co., Ltd.) for 10 min. The remaining steps were the same as for tissue immunofluorescence analysis. The primary antibodies used were as follows: Rabbit anti-collagen type I α1 chain (COL1A1; 1:100 dilution; cat. no. TA7001; Abmart Pharmaceutical Technology Co., Ltd.), rabbit anti-collagen type III α1 chain (COL3A1; 1:100 dilution; cat. no. PS03702; Abmart Pharmaceutical Technology Co., Ltd.), rabbit anti-α smooth muscle actin antibody (1:100 dilution; cat. no. 14395-1-AP; Proteintech Group, Inc.), rabbit anti-Vimentin (1:100 dilution; cat. no. 10366-1-AP; Proteintech Group, Inc.) and mouse anti-E-cadherin (1:100 dilution; cat. no. Sc-8426; Santa Cruz Biotechnology, Inc.). Subsequently, the sections were incubated with the corresponding secondary antibody at 37˚C in the dark for 1 h, washed three times with PBS, stained with DAPI (Beyotime Institute of Biotechnology) for 8 min at room temperature and sealed with anti-fade agent. The secondary antibodies included goat anti-rabbit IgG (H+L) Cross-Adsorbed Secondary Antibody, Alexa Fluor™ 546 (1:500 dilution; A11010; Thermo Fisher Scientific, Inc.) and goat anti-mouse IgG, IgM, IgA (H+L) Secondary Antibody, Alexa Fluor™ 488 (1:10,000 dilution; A10667; Thermo Fisher Scientific, Inc.). All images were obtained and analyzed using a Nikon A1R confocal microscope (Nikon Corporation) with NIS-Elements Viewer 4.5 software (Nikon Corporation).

Cytoskeleton F-actin phalloidin. The tissue specimens were soaked in 4% paraformaldehyde at 4˚C for 24 h. The tissues were then transferred to 30% sucrose solution and left to sink overnight at 4˚C. After embedding with optimal cutting temperature compound (cat. no. 4583; Sakura Finetek USA, Inc.), the tissue blocks were cut into 12-μm-thick sections using a freezing microtome (Leica CM1950; Leica Microsystems GmbH) for immunofluorescence staining. Frozen tissue sections were thawed and washed three times with PBS, permeabilized with 0.3% Triton X-100 in PBS for 5 min at room temperature and washed three times with 0.3% Triton X-100 + 1% BSA (Beyotime Institute of Biotechnology). Subsequently, the sections were incubated with 50 nmol/l FITC-labeled phalloidin (cat. no. RM02836; ABclonal Biotech Co., Ltd.) in the dark for 1 h at room temperature. The sections were washed three times with PBS, and incubated with DAPI solution for 8 min at room temperature to stain the nuclei. Sections were then washed with PBS, and the cells were observed and images were captured under a Nikon A1R confocal microscope (Nikon Corporation).

Western blotting. Proteins were extracted from vaginal wall tissue or fibroblasts using lysis buffer containing protease inhibitors and phosphatase inhibitors (cat. no. KGB5303; Jiangsu Kaiji Biotechnology Co., Ltd.). The protein concentration was determined using a BCA protein assay kit (Jiangsu Kaiji Biotechnology Co., Ltd.). Equal amounts of protein (20 μg/lane) were separated on a 10% SDS-PAGE gel and subsequently transferred to a PVDF membrane (MilliporeSigma). The membrane was then blocked with 5% skim milk for 1 h at room temperature and subsequently incubated with primary antibodies overnight at 4˚C. The membrane was washed three times with TBS with 0.1% Tween (10 min/wash) and incubated with an HRP-labeled goat anti-rabbit or goat anti-mouse secondary antibody (1:10,000 dilution; cat. nos. SA00001-2 and SA00001-1; Proteintech Group, Inc.) for 1 h at room temperature. Protein bands were visualized using ECL (Jiangsu Kaiji Biotechnology Co., Ltd.), and images were captured and analyzed with Image Lab 6.1 software (Bio-Rad Laboratories, Inc.). All experiments were conducted at least three times. The antibodies used for western blotting were anti-collagen I (cat. no. ab138492) and anti-collagen III (cat. no. ab184993) from Abcam, and anti-integrin-β1 (cat. no. A23497), anti-MMP-1 (cat. no. A1191),

anti-TIMP-1 (cat. no. A4959), anti-TGF-β1 (cat. no. A22296) and anti-GAPDH (cat. no. AC033) from ABclonal Biotech Co., Ltd. All antibodies were diluted 1:1,000.

Reverse transcription-quantitative PCR (RT-qPCR). mRNA expression levels of various genes in vaginal wall tissues or fibroblasts were evaluated using RT-qPCR. The primers used for amplification were purchased from Sangon Biotech Co., Ltd., and FreeZol Reagent (R711-01; Vazyme Biotech Co., Ltd.) was used to extract total RNA. Using a PrimeScript™ RT reagent Kit (Takara Bio, Inc.), cDNA was synthesized with 1 μg RNA as a template. The following temperature protocol was used for reverse transcription: 85˚C for 5 sec for the reverse transcription reaction; 37˚C for 15 min to inactivate the reverse transcriptase; and 4˚C to store the reverse transcription product. RT-qPCR was conducted using a SYBR-Green qPCR kit (Takara Bio, Inc) according to the manufaturer's instructions. The thermocycling conditions were as follows: Initial denaturation at 95˚C for 10 min, followed by 40 cycles of 95˚C for 30 sec, 56˚C for 30 sec and 72˚C for 20 sec. Gene expression was normalized to the expression of GAPDH, a housekeeping gene, and mRNA levels were quantified using the $2^{-\Delta\Delta Cq}$ method (25). The primer sequences are shown in Table II.

Table II. Primer sequences of the analyzed genes.

Gene (human)	Sequence (5'-3')
COL3A1-F	TTGAAGGAGGATGTTCCCATCT
COL3A1-R	ACAGACACATATTTGGCATGGTT
COL1A1-F	GAGGGCCAAGACGAAGACATC
COL1A1-R	CAGATCACGTCATCGCACAAC
GAPDH-F	GGAGCGAGATCCCTCCAAAAT
GAPDH-R	GGCTGTTGTCATACTTCTCATGG

COL1A1, collagen type I α1 chain; COL3A1, collagen type III α1 chain; F, forward; ITGB1, integrin subunit β1; R, reverse; TIMP-1, tissue inhibitor of metalloproteinase-1.

Extraction and culture of primary fibroblasts from the anterior vaginal wall. Anterior vaginal wall tissue obtained during surgery was immediately placed in DMEM (Thermo Fisher Scientific, Inc.), and washed with PBS containing 100 U/ml penicillin and 100 mg/ml streptomycin (cat. no. C0222; Beyotime Institute of Biotechnology). The tissue was then cut into small pieces with sterile ophthalmic scissors. Tissues were digested with 0.2% collagenase I (Beijing Solarbio Science & Technology Co., Ltd.) at 37˚C with 5% CO_2 for 12 h and then further digested with 0.25% trypsin (Beijing Solarbio Science & Technology Co., Ltd.) for 3 min at room temperature. Digestion was terminated with 10% fetal bovine serum (cat. no. C04001-500; batch, 2142312; Biological Industries). Fetal bovine serum production quality complied with the Current Good Manufacturing Practice requirements and passed ISO13485: 2016 quality certification. The same batch of fetal bovine serum was used in all cell culture processes. The digested tissue was centrifuged at 350 x g at room temperature for 5 min. The supernatant was discarded, and the cells were resuspended in DMEM (Thermo Fisher Scientific, Inc.) containing 10% fetal bovine serum and 1% (v/v) penicillin-streptomycin (cat. no. C0222; Beyotime Institute of Biotechnology), then cultured in a 5% CO_2-humidified atmosphere at 37˚C. The medium was changed every 2 days. Fibroblasts were used at passages 3-8. The cells were observed using an Olympus BX51 light microscope (Olympus Corporation).

Construction of a mechanical loading model of fibroblasts. Well-growing fibroblasts from the 4th to 8th generations were used to generate the mechanical loading model. Cells were identified as fibroblasts using immunofluorescence staining of cell markers. Primary fibroblasts from the vaginal wall were then seeded into a Bioflex 6-well plate (Flexcell International Corporation) coated with rat tail type I collagen at a density of $3x10^5$ per well and cultured. After the cells reached 80% confluency, the 6-well plate was placed in the second-generation multi-channel cell tensile stress loading system (jointly developed by the Affiliated Hospital of Qingdao Medical University, Qingdao, China, and Ocean University of China, Qingdao, China.). A review of the literature indicated that the mechanical stress of fibroblasts is mostly 8-20% (26). Preliminary experiments set up three gradients of 10, 15 and 20%, and found that there was no significant difference in cells under 10% stress, while the cell death rate was high under 20% stress, and 15% stress more closely simulated the POP state (data not shown). Therefore, 0.1 Hz and 15% mechanical stress were selected for subsequent experiments to act on fibroblasts for 0, 6, 12 and 24 h. The growth status of cells in each group was observed under an inverted fluorescence microscope (Olympus Corporation).

Annexin V-FITC/PI. Apoptosis was assessed using an Annexin V-FITC/PI apoptosis kit (Jiangsu Kaiji Biotechnology Co., Ltd.) according to the manufacturer's protocol. Fibroblast apoptosis was detected by washing fibroblasts twice with PBS, followed by centrifugation at 350 x g for 5 min at room temperature. The cells were resuspended in 500 μl binding buffer, after which 5 μl annexin V-FITC was added, followed by mixing. Subsequently, 5 μl propidium iodide was added, and the cells were incubated at room temperature in the dark for 10 min. A flow cytometer (BD Accuri C6; BD Biosciences) was used to detect the labeled cells and analysis was performed with FlowJo_v10.8.1 Software (Cabit Information Technology Co., Ltd.).

Cell scratch assay. A marker was used to draw a straight line on the outside of the bottom of a 6-well plate. Cells were routinely cultured to 90% confluency. The tip of a 10-μl pipette was used to create vertical scratches on the cell plate. The scratched cells were rinsed with PBS, after which serum-free medium was added, and culture was continued. Images were captured using an inverted fluorescence microscope (Olympus Corporation) at 0 and 12 h, and the cell migration rate was calculated using ImageJ 1.8.0 software (National Institutes of Health).

Statistical analysis. SPSS 25.0 (IBM Corp.) and GraphPad Prism 10.0 statistical software (Dotmatics) were used for data processing and statistical analysis. The results are presented as

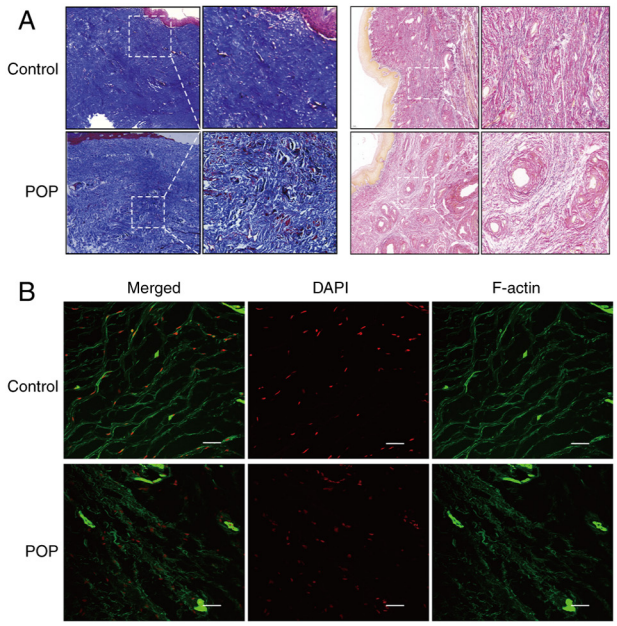

Figure 1. Morphological staining of vaginal wall tissue in the normal and POP groups. (A) Masson's trichrome (left; magnification, x100; magnification of the magnified area, x200) and Elastica van Gieson (right; magnification, x100; magnification of the magnified area, x200) staining of vaginal wall tissues from control subjects and patients with POP. (B) Phalloidin staining of vaginal wall tissues (scale bar, 100 μm) from control subjects and patients with POP. F-actin, filamentous actin; POP, pelvic organ prolapse.

the mean ± SD of at least three independent experiments. For comparisons of two groups, P-values were determined by an unpaired two-tailed Student's t-test, and multiple groups were compared by one-way ANOVA followed by Tukey's multiple comparisons post hoc test. P<0.05 was considered to indicate a statistically significant difference.

Results

Molecular changes in vaginal tissues from patients with POP. Morphological changes in the vaginal wall tissues in the POP group were compared with those in the normal control group. The collagen fibers in the lamina propria in the POP group were loosely arranged and disordered. The elastic fiber density was reduced and broken in several places (Fig. 1A). Analysis of phalloidin staining observed via laser confocal microscopy revealed that the F-actin stress fibers in the normal control group were evenly distributed, dense, continuous and orderly in the form of filaments, whereas the F-actin stress fibers in the POP group were wavy in shape and distinctly distorted, with complete destruction of the structure (Fig. 1B). This suggested that the structural destruction and impairment of the functional integrity of the pelvic floor connective tissue were closely associated with POP.

Expression levels of COL1A1 and COL3A1 are reduced in the vaginal wall tissues of the POP group. To determine the localization and expression levels of collagen in the vaginal wall tissue, immunofluorescence staining was conducted. COL1A1 and COL3A1 were mainly expressed in the cytoplasm, and the fluorescence intensity in the POP group was reduced compared with that in the normal control group (Fig. 2A). RT-qPCR results revealed that, in the prolapsed tissue, the mRNA expression levels of COL1A1 and COL3A1 were relatively high, which may be associated with compensatory gene expression of collagen and disordered elastin fiber structure (Fig. 2B). Western blot analysis revealed that the protein expression levels of COL1A1 and COL3A1 were significantly decreased in tissues from patients with POP compared with tissues from the control group (Fig. 2C; P<0.05).

Changes in the expression levels of integrin-β1, TGF-β1, MMP-1 and tissue inhibitor of metalloproteinase-1 (TIMP-1) in vaginal wall tissue. Western blot analysis revealed that the protein expression levels of integrin-β1, TGF-β1 and TIMP-1 were significantly reduced, and the protein expression levels of MMP-1 were significantly increased in tissues from patients with POP compared with in tissues from the control group (P<0.05; Fig. 3).

Extraction and identification of primary fibroblasts. A type I collagenase digestion method was used to extract cells. Fibroblasts of the 4th passage were selected for immunofluorescence staining. Cells that were negative for E-cadherin and smooth muscle actin but positive for vimentin were considered to be fibroblasts (27) (Fig. 4B). Observation under an inverted microscope revealed that the cells in both the POP group and the control group were spindle-shaped, with clear boundaries, transparent cytoplasm and large nuclei. However, fibroblasts in the POP group were generally longer, and triangular or polygonal cells were less common in the POP group than in the control group (Fig. 4A).

Integrin-β1 inhibitor reduces the migration of fibroblasts, and the expression levels of COL1A1 and COL3A1. Fibroblasts secrete growth factors when migrating at scratches to promote collagen production (28). As shown in Fig. 5A, compared with that in the control group, the migration of fibroblasts was significantly reduced in the integrin-β1 inhibitor group (P<0.05) and non-significantly reduced in the POP group. Flow cytometry revealed that apoptosis was significantly increased in the integrin-β1 inhibitor group and POP group compared with the control group (Fig. 5B). Western blot analysis revealed that after treatment with an integrin-β1 inhibitor, the expression levels of COL1A1, COL3A1 and integrin-β1 in fibroblasts were decreased compared with those in the normal control group (Fig. 5C; P<0.05), indicating that the expression levels of integrin-β1 were closely associated with the expression levels of collagen.

Construction of an in vitro fibroblast stress loading model. To investigate the impact of mechanical force on fibroblasts, a cellular mechanical tensile load model was established. As shown in Fig. 6, when observed under an inverted phase contrast microscope, at 0 h (no mechanical stress) cultured fibroblasts were distributed randomly with disordered growth directions. When 15% mechanical stress was applied to stretch the cells for 6, 12 or 24 h, the morphological differences at 6 h were not obvious; however, after stretching for 12 h, cell adhesion deteriorated and the cells became spindle-shaped. After 24 h of stretching, the fibroblasts were more transparent, with

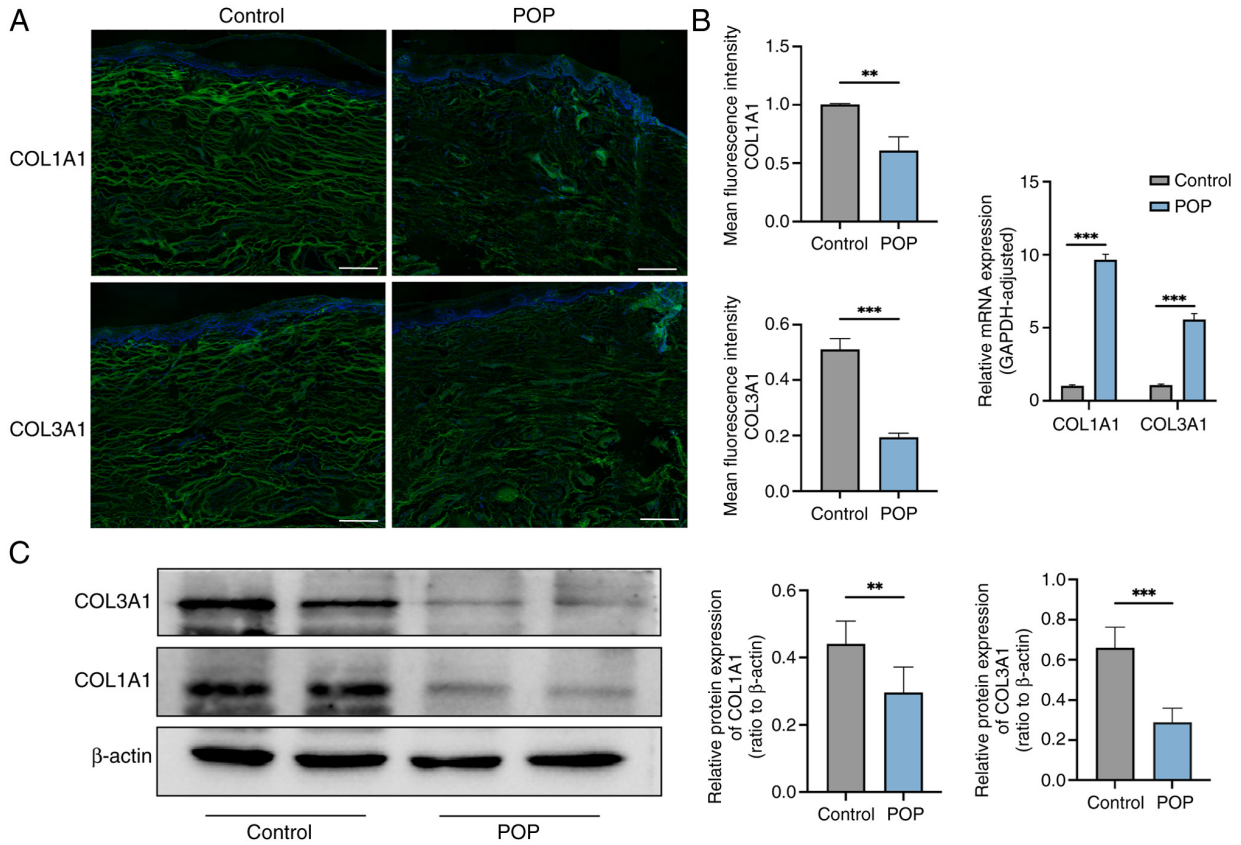

Figure 2. Localization and expression level differences in type I and III collagen in vaginal wall tissues. (A) Immunofluorescence analysis of COL1A1 and COL3A1 expression in the control group and POP group (scale bar, 200 μm). (B) COL1A1 and COL3A1 relative intensity and mRNA expression. (C) COL1A1 and COL3A1 protein immunoblotting and relative protein expression level analysis. **P<0.01 and ***P<0.001 vs. control group. COL1A1, collagen type I α1 chain; COL3A1, collagen type III α1 chain; POP, pelvic organ prolapse.

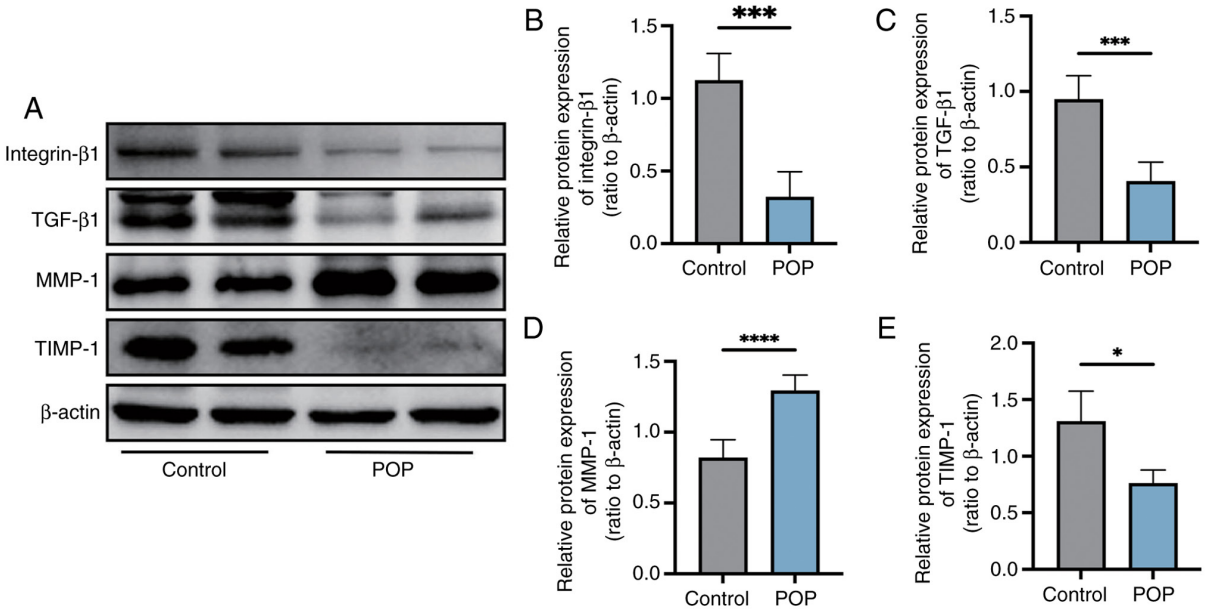

Figure 3. Differences in the protein expression levels of integrin-β1, TGF-β1, MMP-1 and TIMP-1 in vaginal wall tissues. (A) Representative western blot images, and semi-quantification of (B) integrin-β1, (C) TGF-β1, (D) MMP-1 and (E) TIMP-1 protein expression. *P<0.05, ***P<0.001 and ****P<0.0001 vs. control group. POP, pelvic organ prolapse; TIMP-1, tissue inhibitor of metalloproteinase-1.

round cells suspended in the culture medium and adherent cells gradually exhibiting an elongated spindle shape with a tendency to be arranged in neat and consistent directions.

Effects of different stretching times on the expression levels of integrin-β1, and collagen I and III. To further study the effects of different stretching times on fibroblasts,

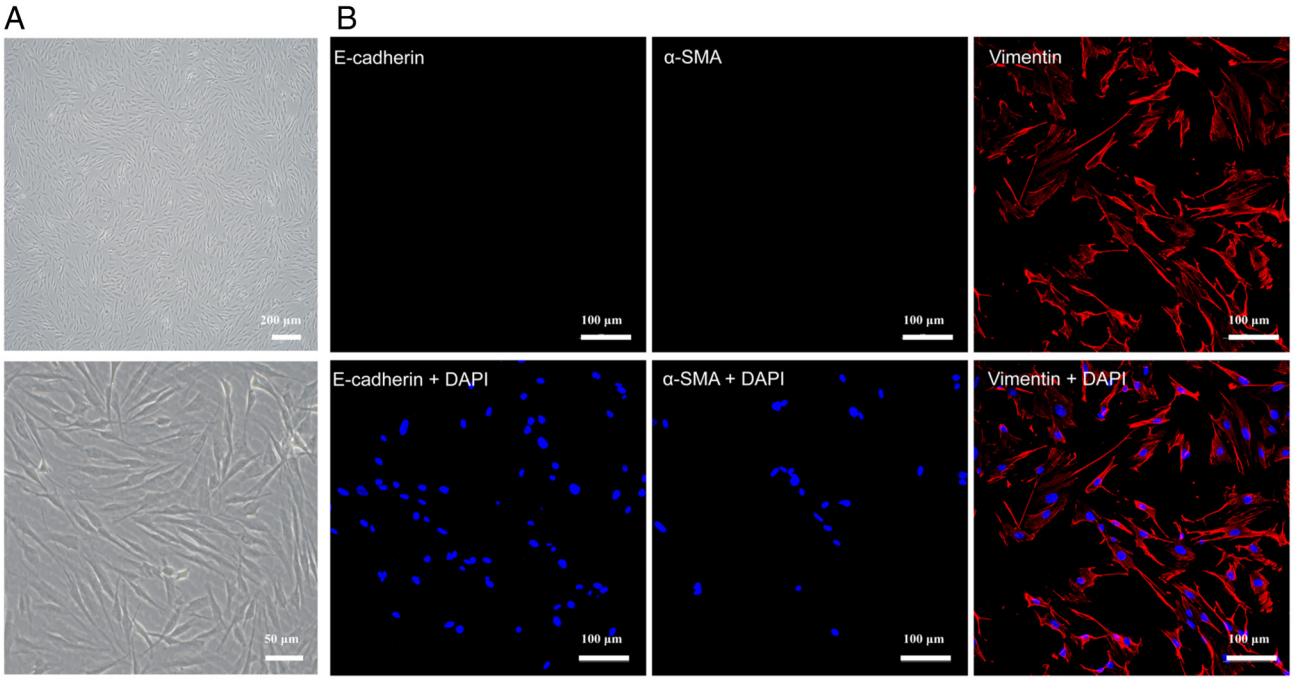

Figure 4. Identification of primary fibroblasts. (A) Fourth-passage fibroblasts under an inverted microscope. Scale bar, 200 μm (top) or 50 μm (bottom). (B) Cellular immunofluorescence staining. Red indicates positive expression of intermediate filament vimentin. Vimentin was localized mainly in the cytoplasm in the form of a fine filament mesh. E-cadherin and α-SMA staining was negative. The cell nuclei were stained with DAPI (blue). Magnification, x20. Scale bar, 100 μm. α-SMA, α-smooth muscle actin.

integrin-β1, COL1A1 and COL3A1 protein levels before and after mechanical stretching for 6, 12 and 24 h were assessed (Fig. 7). Compared with those in non-stretched cells (0 h), the protein expression levels of integrin-β1 and COL3A1 were decreased in cells after stretching for 6 h, although not significantly, and collagen I expression was significantly decreased. However, the expression levels of COL1A1 and COL3A1 were significantly increased after stretching for 12 h. After 24 h, there was no significant difference in the expression levels of integrin-β1, COL1A1 and COL3A1 compared with the unstretched group (0 h).

Annexin V-FITC/PI assessment of changes in the apoptosis rate of fibroblasts. Analysis of flow cytometry results revealed that the apoptosis rate of fibroblasts increased with prolonged cyclic tensile stress loading deformation between 0 and 24 h (Fig. 8). In summary, there was a positive association between the apoptosis rate of fibroblasts and the mechanical loading and stretching time.

Western blot analysis of the protein expression levels of collagen, integrin-β1, TGF-β1, TIMP-1 and MMP-1 in different treatment groups. Western blot analysis revealed that, after applying 15% mechanical force for 12 h, integrin-β1 expression was increased compared with that in the control group (Fig. 9). Furthermore, the expression levels of TIMP-1, COL1A1 and COL3A1 were increased, whereas the expression levels of TGF-β1 and MMP-1 were decreased. Following addition of integrin-β1 inhibitor, compared with the control group without addition of inhibitor, the expression levels of integrin-β1, TGF-β1, TIMP-1, COL1A1 and COL3A1 were lower, whereas the expression levels of MMP-1 were higher. In addition, when integrin inhibitors were added and mechanical force stimulation was applied at the same time, compared with those in the group in which only mechanical force was applied, the expression levels of TGF-β1, COL1A1 and COL3A1 were lower, while the expression levels of MMP-1 and TIMP-1 were higher. Following addition of integrin inhibitors and application of mechanical force stimulation compared with the normal control group, the expression levels COL1A1, MMP-1 and TIMP-1 were increased, the expression levels of integrin-β1 and TGF-β1 were decreased, and there was no significant change in COL3A1 expression.

Discussion

POP, which refers to the abnormal position and function of pelvic organs caused by weak pelvic floor support tissue, has a marked effect on the physical and mental health of women, leading to a reduction in the quality of life (29). The pelvic floor connective tissue, which is primarily composed of the ECM, including collagen, elastin and proteoglycans, serves a key role in the pelvic support structure (30). Collagen, the main component of the ECM (29), strongly influences the function of the pelvic floor connective tissue through its content and fiber arrangement. Additionally, vaginal smooth muscle bundles are responsible for vaginal muscle tone and contraction, and are closely associated with organ function (31). Numerous studies have reported differences in the collagen content and proportion in the pelvic floor support tissues of patients with POP compared with individuals with other benign gynecological conditions who do not have POP (32,33). However, to the best of our knowledge, the exact changes in collagen are unclear. In the present

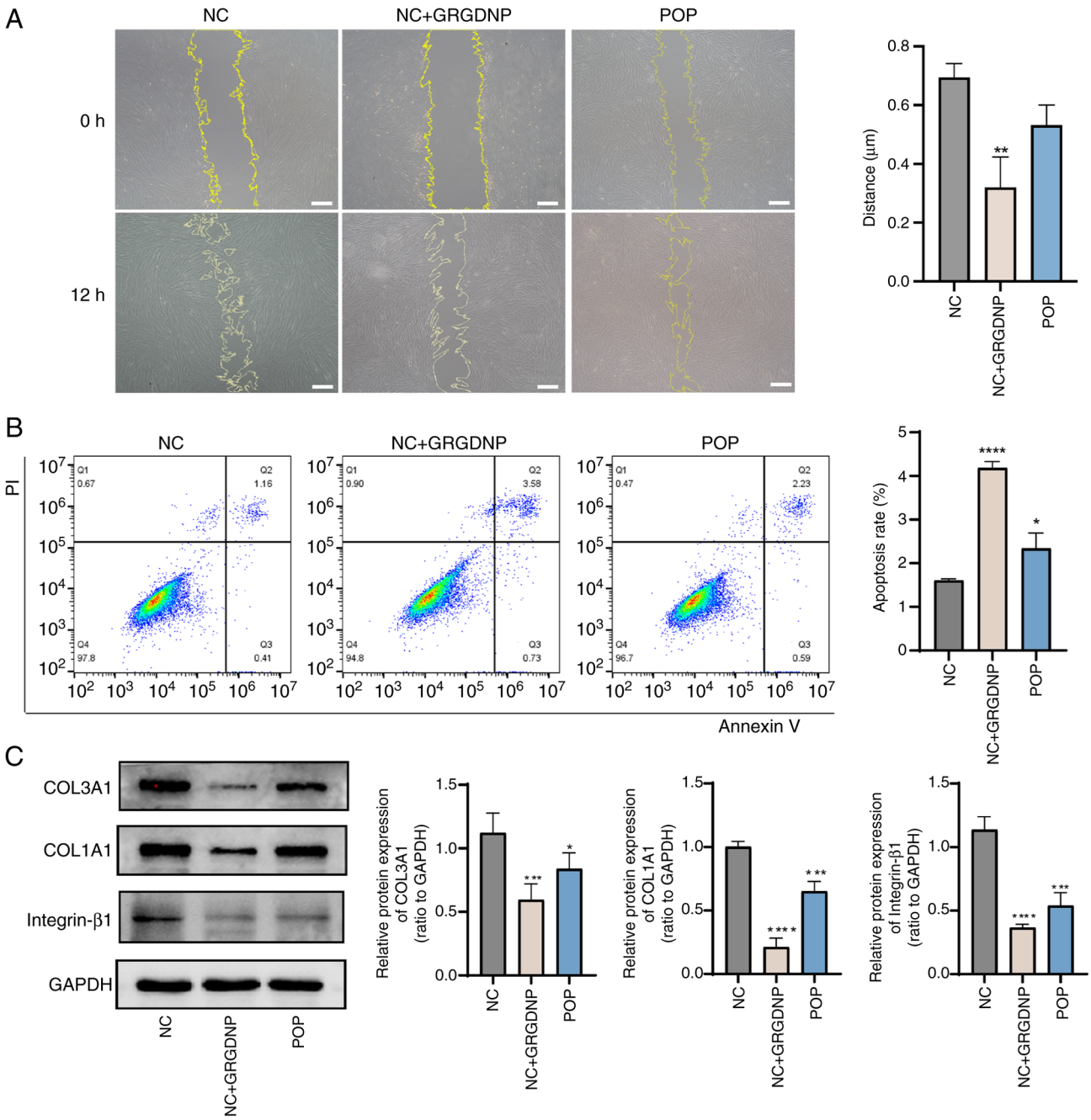

Figure 5. Effects of integrin-β1 antagonist on fibroblast migration, apoptosis and protein expression. (A) Images of the cell scratch experiment and quantitative analysis. Scale bar, 200 μm. (B) Fibroblasts were stained using an annexin V-FITC/PI staining kit and analyzed by flow cytometry. (C) Protein immunoblotting and relative protein expression levels. *P<0.05, **P<0.01, ***P<0.001 and ****P<0.0001 vs. normal control group. COL1A1, collagen type I α1 chain; COL3A1, collagen type III α1 chain; GRGDNP, RGD peptide; NC, negative control; POP, pelvic organ prolapse.

study, Masson's trichrome staining and EVG staining were used to examine the collagen fiber structure of the vaginal wall tissues of patients with POP. The findings aligned with previous studies that discussed a looser and more disordered collagen fiber structure, along with multiple breaks in elastic fibers in patients with POP (34,35). These results suggest that reduced collagen and elastin contents, as well as the disruption of the structural integrity of pelvic floor connective tissues were associated with POP. However, the molecular mechanisms underlying abnormal ECM metabolism in the pelvic floor connective tissues of patients with POP are not yet fully understood.

In addition to being influenced by age-associated degeneration, female pelvic floor tissues are influenced by various forces, such as gravity, pregnancy, childbirth, coughing and defecation (36). A study has confirmed that the biomechanical properties of cells in the pelvic floor support tissues of patients with POP are abnormal (37). This suggests that POP may result from a decrease in the biomechanical properties of pelvic floor support tissues (38). Cytoskeletal remodeling is a key process in which cells respond to mechanical stimulation (39). Integrins serve a key role in forming tension-dependent connections between the ECM and the cytoskeleton; they are essential for converting mechanical forces into biochemical

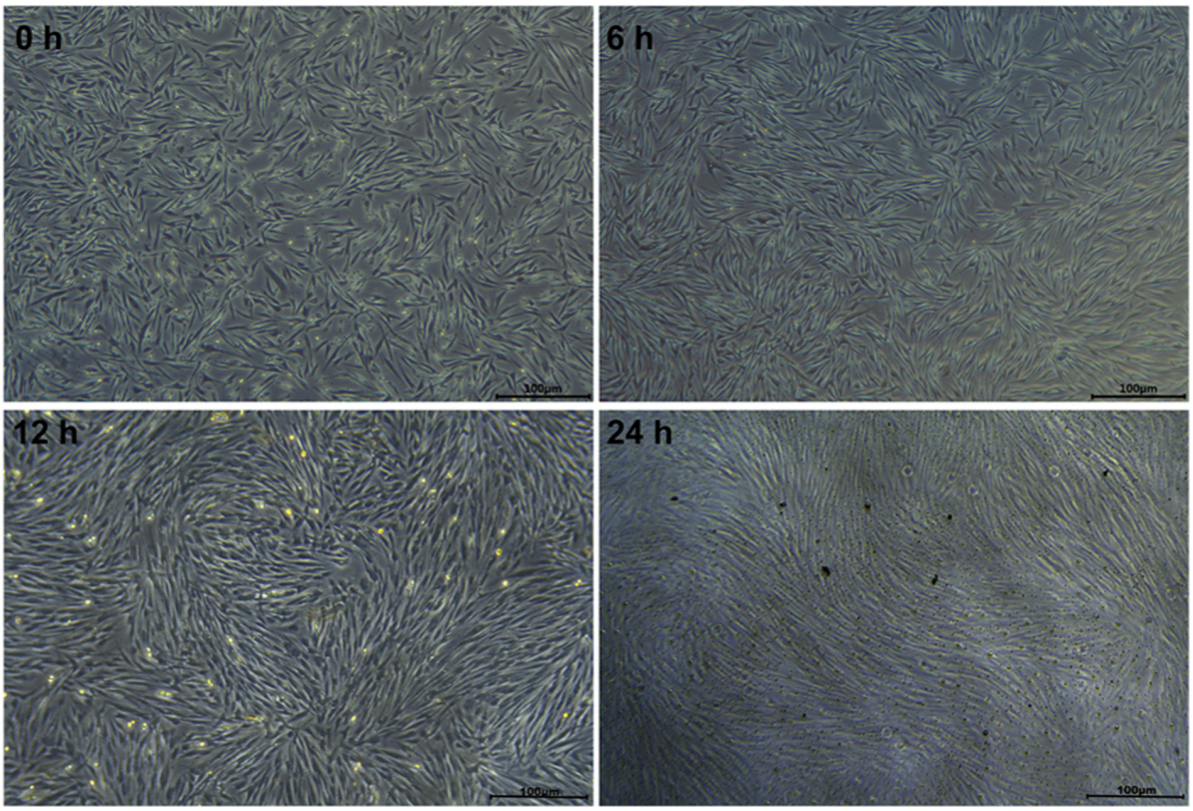

Figure 6. Morphological changes in fibroblasts under 15% tensile stress for 0, 6, 12 and 24 h, as observed under an inverted phase contrast microscope. Scale bar, 100 μm.

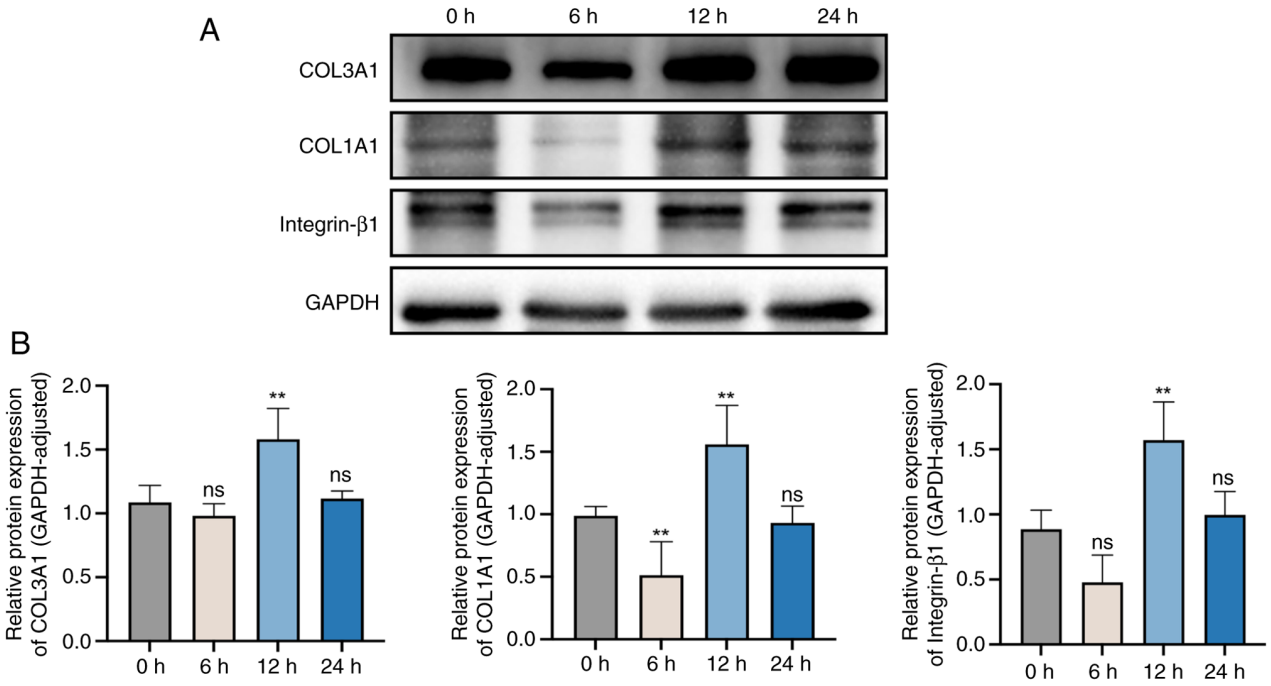

Figure 7. Effects of different stretching times on the expression levels of integrin-β1 and collagen I and III. (A) Representative protein immunoblots and (B) semi-quantified expression levels of proteins. **P<0.01 vs. control (0 h) group. COL1A1, collagen type I α1 chain; COL3A1, collagen type III α1 chain; ns, not significant.

signals (40). Additionally, TGF-β1 is important for regulating the conversion of ECM components (41); it promotes collagen synthesis and inhibits its degradation, thus maintaining the structure and function of the pelvic floor connective tissue. MMPs are enzymes that degrade ECM components, whereas TIMP-1 specifically inhibits MMPs (22). TIMP-1, a member

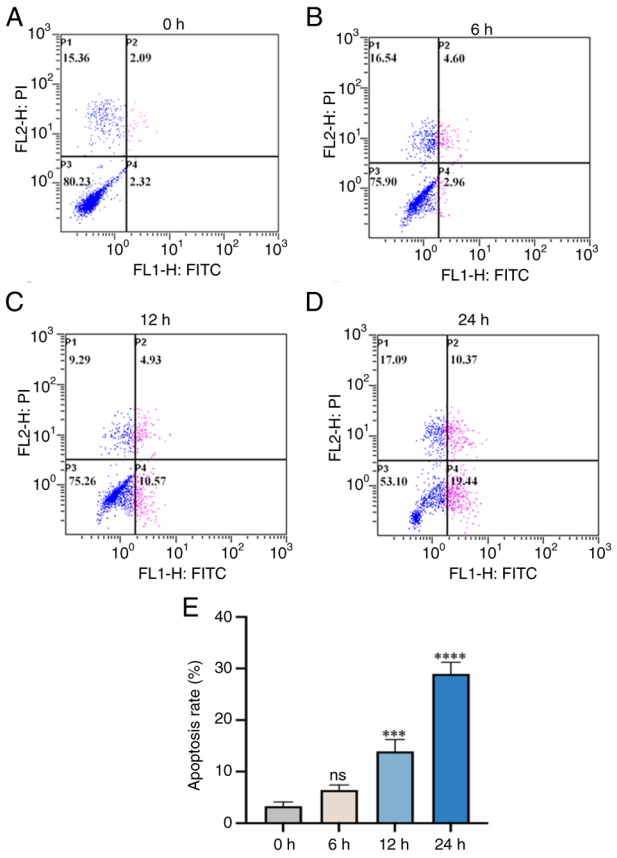

Figure 8. Flow cytometry was used to detect apoptotic cells in groups treated with 15% tensile stress for (A) 0, (B) 6, (C) 12 and (D) 24 h. (E) Quantification of the apoptosis rate. ***P<0.001 and ****P<0.0001 vs. control (0 h) group. ns, not significant.

of the TIMP family, is present in body fluids and tissues; it inhibits the binding of various MMPs to ECM components, thereby preventing the degradation of collagen and maintaining the balance of ECM components in normal connective tissue (42). Previous research has revealed that the signaling pathways mediated by integrins and TGF-β receptors not only share some signaling molecules but also have synergistic effects and promote each other. For example, in fibrotic diseases, TGF-β1 induces integrin expression, whereas inhibiting integrin expression reduces TGF-β1-mediated collagen synthesis (43,44).

Studies have shown that female patients with POP exhibit decreased expression levels of COL1A1 in vaginal wall tissues, whereas the total amount of COL3A1 is increased (45-47). In the present study, fibroblasts were from the lamina propria of the vaginal wall. In the POP group, COL1A1 and COL3A1 protein levels were lower. However, one study found less COL1A1 but more COL3A1 in the muscular layer. This contradiction may be due to different sampling sites (46). Additionally, the expression levels of integrin-β1, TGF-β1 and TIMP-1 were decreased in the POP group compared with the control group, while the expression levels of MMP-1 were increased; these differences were found to be statistically significant. It can be hypothesized that the reduced expression levels of integrin-β1/TGF-β1 in the pathogenesis of POP inhibit the activity of TIMP-1, leading to a decrease in its inhibitory effect on MMP-1 activity and the subsequent degradation of ECM proteins such as collagen. The loss of collagen weakens the supporting tissues of the pelvic floor (48). To test this hypothesis, primary fibroblasts were extracted and treated with an integrin-β1 inhibitor. The results revealed reduced migration, an increased apoptosis rate, decreased expression levels of TGF-β1, TIMP-1, COL1A1 and COL3A1 and significantly increased expression levels of MMP-1 compared with those in the normal control group (P<0.05).

To investigate whether mechanical force regulates ECM metabolism in pelvic floor connective tissues through the integrin-β1-mediated signaling pathway, in the present study, mechanical stimulation and a mechanical damage loading model of fibroblasts were established. Fibroblasts were subjected to mechanical forces with the same stretch amplitude and frequency but different durations. Over time, the fibroblasts gradually assumed an elongated spindle shape with a neat and consistent arrangement, while the apoptosis rate increased. Therefore, we hypothesized that mechanical stretch induces fibroblast apoptosis by damaging the actin cytoskeleton, a process that is associated with mechanical stretch-induced actin cytoskeleton remodeling (49,50). At 12 h, the fibroblast cytoskeleton underwent mechanical stretching, resulting in an increase in the expression levels of integrin-β1. Furthermore, there was an increase in the levels of TIMP-1, COL1A1 and COL3A1, accompanied by a decrease in TGF-β1 and MMP-1. Upon applying an inhibitor of integrin-β1 and subjecting the cells to the same mechanical force stimulation, a comparison with cells treated with 15% stress in the absence of the inhibitor revealed a decrease in the expression levels of integrin-β1, COL1A1 and COL3A1. Additionally, an increase in the expression levels of MMP-1 and TIMP-1 was observed, while no significant change in TGF-β1 levels was noted. These findings indicated that mechanical force could influence the expression levels of integrin-β1, which is located in the cytoskeleton, leading to aberrant cellular signal transduction and affecting the levels of TGF-β1, TIMP-1 and MMP-1. Additionally, mechanical stimulation increased the apoptosis rate of fibroblasts. At the beginning of loading, the cytoskeleton was destroyed by mechanical force, and the expression of type I collagen decreased, while type III collagen did not change significantly. With the extension of mechanical loading time, the expression of type I and type III collagen increased. Finally, when the mechanical stimulation exceeded a certain time (24 h), the cells appeared to adapt to the mechanical stimulation, and the expression of type I and type III collagen decreased. The results showed that under a certain range of mechanical stress, the synthetic function of fibroblasts was enhanced, the anabolism and catabolism of collagen were increased, and the extracellular matrix was remodeled.

In the present study, an integrin-β1 inhibitor was used to examine the expression levels of TGF-β1 and its downstream signaling molecules. To further investigate the interaction between integrin-β1 and TGF-β1, the expression levels of TGF-β1 will be manipulated in future experiments, allowing the investigation of dynamic changes in integrin-β1 and the corresponding alterations in ECM protein expression levels.

Additionally, the present study had limitations, particularly regarding the cell stress loading model, where only cyclic cell stretching was used. Given that the human body is influenced by gravitational forces, this periodic force does not adequately

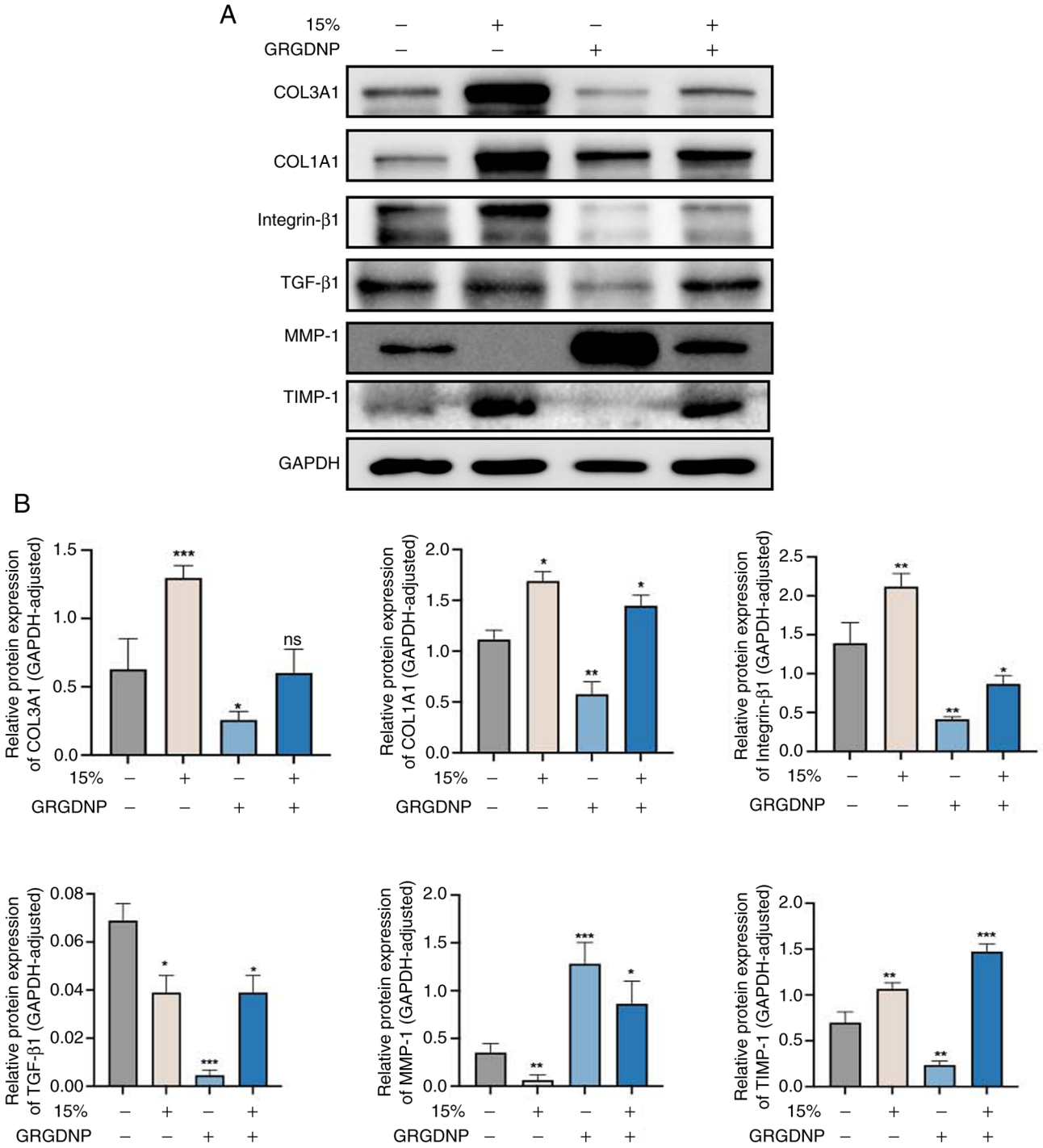

Figure 9. Western blot analysis of protein expression levels in different treatment groups. (A) Representative protein immunoblots and (B) semi-quantified expression levels of proteins in cells under 15% tensile stress for 12 h. *P<0.05, **P<0.01 and ***P<0.001 vs. control group (15% force not applied and GRGDNP not applied). COL1A1, collagen type I α1 chain; COL3A1, collagen type III α1 chain; ns, not significant; GRGDNP, RGD peptide; TIMP-1, tissue inhibitor of metalloproteinase-1.

replicate the mechanical stresses experienced *in vivo*. Consequently, future studies will compare fibroblast performance under continuous stretching versus cyclic stretching conditions to assess variations in ECM protein composition. Furthermore, future efforts will focus on identifying the molecular targets regulated by the integrin-β1/TGF-β1 signaling pathway to develop effective diagnostic markers or therapeutic interventions, thereby enhancing the clinical relevance of the present research. Due to challenges in recruiting and following up patients suffering from POP, the sample size in the present study was relatively small. In future studies, an increased sample size will be obtained using multi-center collaborations to further validate and strengthen the findings.

In summary, the disruption of the structural integrity of pelvic floor connective tissues, including collagen and elastin, was closely associated with POP. The downregulation of integrin-β1 expression may be associated with the occurrence and progression of POP. Integrin-β1 served a role in fibroblast

migration, apoptosis and collagen synthesis. Mechanical force can activate the integrin-β1/TGF-β1-mediated signaling pathway within 12 h, leading to increased collagen synthesis and contributing to the development of POP. The present study provides a theoretical foundation for further investigations into the pathogenesis of POP and offers novel targets and approaches for the prevention and treatment of POP.

Acknowledgements

Not applicable.

Funding

The present study was supported by the Ningxia Hui Autonomous Region Science and Technology Benefit People Project (grant no. 2023CMG03027), Ningxia Hui Autonomous Region Key Research and Development Program (grant no. 2022BEG03167) and the National Natural Science Foundation of China (grant no. 82060275).

Availability of data and materials

The data generated in the present study may be requested from the corresponding author.

Authors' contributions

MK, YL and ZW conceived the present study and established the initial design of the present study. MK and ZW wrote the manuscript. MK, ZW, YH, YS, XY and NRD conducted the experiments and analyzed the data. YL revised the manuscript. YL and MK confirm the authenticity of all the raw data. All authors have read and approved the final manuscript.

Ethics approval and consent to participate

All procedures involving human samples in the present study were conducted with ethics-approved protocols in accordance with the guidelines of the Ethics Committee of Ningxia Medical University (approval no. KYLL-2024-0223; Yinchuan, China). All patients provided written informed consent before surgery.

Patient consent for publication

Not applicable.

Competing interests

The authors declare that they have no competing interests.

References

1. Weintraub AY, Glinter H and Marcus-Braun N: Narrative review of the epidemiology, diagnosis and pathophysiology of pelvic organ prolapse. Int Braz J Urol 46: 5-14, 2020.
2. Buchsbaum GM, Duecy EE, Kerr LA, Huang LS, Perevich M and Guzick DS: Pelvic organ prolapse in nulliparous women and their parous sisters. Obstet Gynecol 108: 1388-1393, 2006.
3. Jelovsek JE, Maher C and Barber MD: Pelvic organ prolapse. Lancet 369: 1027-1038, 2007.
4. Iglesia CB and Smithling KR: Pelvic organ prolapse. Am Fam Physician 96: 179-185, 2017.
5. Friedman T, Eslick GD and Dietz HP: Risk factors for prolapse recurrence: Systematic review and meta-analysis. Int Urogynecol J 29: 13-21, 2018.
6. Altman D, Zetterstrom J, Schultz I, Nordenstam J, Hjern F, Lopez A and Mellgren A: Pelvic organ prolapse and urinary incontinence in women with surgically managed rectal prolapse: A population-based case-control study. Dis Colon Rectum 49: 28-35, 2006.
7. Slieker-ten Hove MC, Pool-Goudzwaard AL, Eijkemans MJ, Steegers-Theunissen RP, Burger CW and Vierhout ME: The prevalence of pelvic organ prolapse symptoms and signs and their relation with bladder and bowel disorders in a general female population. Int Urogynecol J Pelvic Floor Dysfunct 20: 1037-1045, 2009.
8. Pang H, Zhang L, Han S, Li Z, Gong J, Liu Q, Liu X, Wang J, Xia Z, Lang J, *et al*: A nationwide population-based survey on the prevalence and risk factors of symptomatic pelvic organ prolapse in adult women in China - A pelvic organ prolapse quantification system-based study. BJOG 128: 1313-1323, 2021.
9. Smith FJ, Holman CD, Moorin RE and Tsokos N: Lifetime risk of undergoing surgery for pelvic organ prolapse. Obstet Gynecol 116: 1096-1100, 2010.
10. Wu JM, Matthews CA, Conover MM, Pate V and Jonsson Funk M: Lifetime risk of stress urinary incontinence or pelvic organ prolapse surgery. Obstet Gynecol 123: 1201-1206, 2014.
11. Wu JM, Kawasaki A, Hundley AF, Dieter AA, Myers ER and Sung VW: Predicting the number of women who will undergo incontinence and prolapse surgery, 2010 to 2050. Am J Obstet Gynecol 205: 230.e1-5, 2011.
12. Schulten SFM, Claas-Quax MJ, Weemhoff M, van Eijndhoven HW, van Leijsen SA, Vergeldt TF, IntHout J and Kluivers KB: Risk factors for primary pelvic organ prolapse and prolapse recurrence: An updated systematic review and meta-analysis. Am J Obstet Gynecol 227: 192-208, 2022.
13. Flusberg M, Kobi M, Bahrami S, Glanc P, Palmer S, Chernyak V, Kanmaniraja D and El Sayed RF: Multimodality imaging of pelvic floor anatomy. Abdom Radiol (NY) 46: 1302-1311, 2021.
14. Ruiz-Zapata AM, Heinz A, Kerkhof MH, van de Westerlo-van Rijt C, Schmelzer CEH, Stoop R, Kluivers KB and Oosterwijk E: Extracellular matrix stiffness and composition regulate the myofibroblast differentiation of vaginal fibroblasts. Int J Mol Sci 21: 4762, 2020.
15. Eckes B, Zweers MC, Zhang ZG, Hallinger R, Mauch C, Aumailley M and Krieg T: Mechanical tension and integrin alpha 2 beta 1 regulate fibroblast functions. J Investig Dermatol Symp Proc 11: 66-72, 2006.
16. Becchetti A, Petroni G and Arcangeli A: Ion channel conformations regulate integrin-dependent signaling. Trends Cell Biol 29: 298-307, 2019.
17. Kolasangiani R, Bidone TC and Schwartz MA: Integrin conformational dynamics and mechanotransduction. Cells 11: 3584, 2022.
18. Galliher AJ and Schiemann WP: Beta3 integrin and Src facilitate transforming growth factor-beta mediated induction of epithelial-mesenchymal transition in mammary epithelial cells. Breast Cancer Res 8: R42, 2006.
19. Chen X, Wang H, Liao HJ, Hu W, Gewin L, Mernaugh G, Zhang S, Zhang ZY, Vega-Montoto L, Vanacore RM, *et al*: Integrin-mediated type II TGF-β receptor tyrosine dephosphorylation controls SMAD-dependent profibrotic signaling. J Clin Invest 124: 3295-3310, 2014.
20. Sarrazy V, Koehler A, Chow ML, Zimina E, Li CX, Kato H, Caldarone CA and Hinz B: Integrins αvβ5 and αvβ3 promote latent TGF-β1 activation by human cardiac fibroblast contraction. Cardiovasc Res 102: 407-417, 2014.
21. Perrucci GL, Barbagallo VA, Corlianò M, Tosi D, Santoro R, Nigro P, Poggio P, Bulfamante G, Lombardi F and Pompilio G: Integrin αvβ5 in vitro inhibition limits pro-fibrotic response in cardiac fibroblasts of spontaneously hypertensive rats. J Transl Med 16: 352, 2018.
22. Liu C, Wang Y, Li BS, Yang Q, Tang JM, Min J, Hong SS, Guo WJ and Hong L: Role of transforming growth factor β-1 in the pathogenesis of pelvic organ prolapse: A potential therapeutic target. Int J Mol Med 40: 347-356, 2017.
23. Wang S, Zhang Z, Lü D and Xu Q: Effects of mechanical stretching on the morphology and cytoskeleton of vaginal fibroblasts from women with pelvic organ prolapse. Int J Mol Sci 16: 9406-9419, 2015.
24. Belayneh T, Gebeyehu A, Adefris M, Rortveit G and Genet T: Validation of the amharic version of the pelvic organ prolapse symptom score (POP-SS). Int Urogynecol J 30: 149-156, 2019.

25. Livak KJ and Schmittgen TD: Analysis of relative gene expression data using real-time quantitative PCR and the 2(-Delta Delta C(T)) method. Methods 25: 402-408, 2001.
26. Boccafoschi F, Sabbatini M, Bosetti M and Cannas M: Overstressed mechanical stretching activates survival and apoptotic signals in fibroblasts. Cells Tissues Organs 192: 167-176, 2010.
27. Chen R, Dawson DW, Pan S, Ottenhof NA, de Wilde RF, Wolfgang CL, May DH, Crispin DA, Lai LA, Lay AR, *et al*: Proteins associated with pancreatic cancer survival in patients with resectable pancreatic ductal adenocarcinoma. Lab Invest 95: 43-55, 2015.
28. Landén NX, Li D and Ståhle M: Transition from inflammation to proliferation: A critical step during wound healing. Cell Mol Life Sci 73: 3861-3885, 2016.
29. Collins S and Lewicky-Gaupp C: Pelvic organ prolapse. Gastroenterol Clin North Am 51: 177-193, 2022.
30. Ying W, Hu Y and Zhu H: Expression of CD44, transforming growth factor-β, and matrix metalloproteinases in women with pelvic organ prolapse. Front Surg 9: 902871, 2022.
31. Babinski M, Pires LAS, Fonseca Junior A, Manaia JHM and Babinski MA: Fibrous components of extracellular matrix and smooth muscle of the vaginal wall in young and postmenopausal women: Stereological analysis. Tissue Cell 74: 101682, 2022.
32. Alperin M and Moalli PA: Remodeling of vaginal connective tissue in patients with prolapse. Curr Opin Obstet Gynecol 18: 544-550, 2006.
33. Tian Z, Li Q, Wang X and Sun Z: The difference in extracellular matrix metabolism in women with and without pelvic organ prolapse: A systematic review and meta-analysis. BJOG 131: 1029-1041, 2024.
34. Tola EN, Koroglu N, Yıldırım GY and Koca HB: The role of ADAMTS-2, collagen type-1, TIMP-3 and papilin levels of uterosacral and cardinal ligaments in the etiopathogenesis of pelvic organ prolapse among women without stress urinary incontinence. Eur J Obstet Gynecol Reprod Biol 231: 158-163, 2018.
35. Chen B and Yeh J: Alterations in connective tissue metabolism in stress incontinence and prolapse. J Urol 186: 1768-1772, 2011.
36. Gedefaw G and Demis A: Burden of pelvic organ prolapse in Ethiopia: A systematic review and meta-analysis. BMC Womens Health 20: 166, 2020.
37. Zeng W, Li Y, Li B, Liu C, Hong S, Tang J and Hong L: Mechanical stretching induces the apoptosis of parametrial ligament fibroblasts via the actin cytoskeleton/Nr4a1 signalling pathway. Int J Med Sci 17: 1491-1498, 2020.
38. Huntington A, Donaldson K and De Vita R: Contractile properties of vaginal tissue. J Biomech Eng 142: 080801, 2020.
39. Khomtchouk BB, Lee YS, Khan ML, Sun P, Mero D and Davidson MH: Targeting the cytoskeleton and extracellular matrix in cardiovascular disease drug discovery. Expert Opin Drug Discov 17: 443-460, 2022.
40. Li X and Wang J: Mechanical tumor microenvironment and transduction: Cytoskeleton mediates cancer cell invasion and metastasis. Int J Biol Sci 16: 2014-2028, 2020.
41. Carlin GL, Bodner K, Kimberger O, Haslinger P, Schneeberger C, Horvat R, Kölbl H, Umek W and Bodner-Adler B: The role of transforming growth factor-β (TGF-β1) in postmenopausal women with pelvic organ prolapse: An immunohistochemical study. Eur J Obstet Gynecol Reprod Biol X 7: 100111, 2020.
42. Cheng Q, Li C, Yang CF, Zhong YJ, Wu D, Shi L, Chen L, Li YW and Li L: Methyl ferulic acid attenuates liver fibrosis and hepatic stellate cell activation through the TGF-β1/Smad and NOX4/ROS pathways. Chem Biol Interact 299: 131-139, 2019.
43. Madison J, Wilhelm K, Meehan DT, Delimont D, Samuelson G and Cosgrove D: Glomerular basement membrane deposition of collagen α1(III) in Alport glomeruli by mesangial filopodia injures podocytes via aberrant signaling through DDR1 and integrin α2β1. J Pathol 258: 26-37, 2022.
44. Zou GL, Zuo S, Lu S, Hu RH, Lu YY, Yang J, Deng KS, Wu YT, Mu M, Zhu JJ, *et al*: Bone morphogenetic protein-7 represses hepatic stellate cell activation and liver fibrosis via regulation of TGF-β/Smad signaling pathway. World J Gastroenterol 25: 4222-4234, 2019.
45. Sferra R, Pompili S, D'Alfonso A, Sabetta G, Gaudio E, Carta G, Festuccia C, Colapietro A and Vetuschi A: Neurovascular alterations of muscularis propria in the human anterior vaginal wall in pelvic organ prolapse. J Anat 235: 281-288, 2019.
46. Vetuschi A, D'Alfonso A, Sferra R, Zanelli D, Pompili S, Patacchiola F, Gaudio E and Carta G: Changes in muscularis propria of anterior vaginal wall in women with pelvic organ prolapse. Eur J Histochem 60: 2604, 2016.
47. De Landsheere L, Munaut C, Nusgens B, Maillard C, Rubod C, Nisolle M, Cosson M and Foidart JM: Histology of the vaginal wall in women with pelvic organ prolapse: A literature review. Int Urogynecol J 24: 2011-2020, 2013.
48. Montoya TI, Maldonado PA, Acevedo JF and Word RA: Effect of vaginal or systemic estrogen on dynamics of collagen assembly in the rat vaginal wall. Biol Reprod 92: 43, 2015.
49. Zhu Y, Li L, Xie T, Guo T, Zhu L and Sun Z: Mechanical stress influences the morphology and function of human uterosacral ligament fibroblasts and activates the p38 MAPK pathway. Int Urogynecol J 33: 2203-2212, 2022.
50. Saatli B, Kizildag S, Cagliyan E, Dogan E and Saygili U: Alteration of apoptosis-related genes in postmenopausal women with uterine prolapse. Int Urogynecol J 25: 971-977, 2014.